https://doi.org/10.5194/egusphere-2026-2323
Preprint. Discussion started: 11 May 2026

A workflow for the identification of earthquake sources from macroseismic data

Veronica Gironelli[1], Lucia Luzi[1], Andrea Antonucci[1], Andrea Rovida[1]

[1] Istituto Nazionale di Geofisica e Vulcanologia (INGV), Milano, Italy

Correspondence to: Veronica Gironelli (veronica.gironelli@ingv.it)

Abstract. Macroseismic intensity data are a fundamental source of information for characterising historical earthquakes. This study presents a methodology to constrain the sources of large earthquake through the analysis and modelling of macroseismic intensity data. The proposed workflow consists of three main stages: (1) the identification and removal of outlier intensity data points; (2) the revision of macroseismic earthquake parameters (epicentral location and magnitude); and (3) the construction of three-dimensional (3D) seismogenic sources, simulation of ground shaking including site effects, and a subsequent residual analysis. The application of this workflow to a set of case studies from the parametric catalogue of Italian earthquakes demonstrates that the implemented approach allows the identification of seismogenic sources for large to moderate magnitude events, which are consistent with macroseismic data, geological structures and ground motion data, when available. The results of this study can have direct implications for seismic hazard assessment and shaking scenario modelling. The proposed workflow can be systematically applied to reconstruct the seismogenic sources of the strongest Italian historical earthquakes (Mw ≥ 5.5).

1 Introduction

Macroseismic intensity is used to classify the level of shaking caused by earthquakes based on qualitative observations of its effects on people, buildings, and the environment, using standardised intensity scales (e.g., MCS, Sieberg, 1932; MSK, Medvedev et al., 1964; EMS-98, Grünthal, 1998). Among these, the Mercalli–Cancani–Sieberg (MCS) scale and the European Macroseismic Scale 1998 (EMS-98) are the most widely adopted in Italy. These scales consist of twelve intensity degrees, each representing increasing severity of ground shaking based on observed effects. Macroseismic intensity is associated with a specific earthquake and site through geographic coordinates and constitutes a macroseismic Intensity Data Point (IDP).

Macroseismic observations are widely used in earthquake engineering applications for vulnerability modelling and for the calibration of Intensity Prediction Equations (hereafter, IPEs, e.g., Pasolini et al., 2008; Sørensen et al., 2009; Bindi et al., 2011; Rotondi et al., 2016; Gomez-Capera et al., 2024; Lolli et al., 2024), which estimate the expected macroseismic intensity at any site based on parameters such as epicentral distance and magnitude. Similarly, these data are used as input to develop Ground Motion to Intensity Conversion Equations for a specific region (GMICEs, e.g., Gomez-Capera et al., 2020; Oliveti et al., 2022), which relate ground motion Intensity Measures (IMs) to macroseismic intensities or vice versa. In this framework, macroseismic data are also used as a reference for reconstructing the ground shaking distribution of pre-instrumental events (e.g., Allen et al., 2008; Faenza et al., 2013; Oliveti et al., 2024; Gironelli et al., 2023; Munafò et al., 2024; Volatili et al., 2025). Moreover, the spatial distribution of IDPs (i.e., the macroseismic field) enables the estimation of key earthquake parameters such as epicentral location, magnitude, depth, and even the physical dimensions and orientation of seismic ruptures associated with large events (e.g., Gasperini and Ferrari, 1995, 2000; Bakun and Wentworth, 1997; Pettenati et al, 1999; Gasperini et al., 1999, 2010; Provost and Scotti, 2020; Sbarra et al., 2019; 2023).

In Italy, IDPs are systematically collected and organised in the Italian Macroseismic Database (Database Macrosismico Italiano - DBMI15; Locati et al., 2022), to provide a homogeneous dataset

https://doi.org/10.5194/egusphere-2026-2323
Preprint. Discussion started: 11 May 2026

for assessing earthquake parameters and compiling the Italian Parametric Earthquake Catalogue (Catalogo Parametrico dei Terremoti Italiani - CPTI15; Rovida et al., 2020, 2022). In the CPTI15 catalogue, the parameterization of historical events is based on the intensity dataset selected among those archived in the Italian Archive of Historical Earthquake Data (ASMI; Rovida et al., 2017, 2025) according to quality criteria such as: (i) the completeness and spatial distribution of IDPs; (ii) the methodological robustness of the original study; and (iii) the reliability of the event interpretation (Locati et al., 2022).

Given the extensive availability of high-quality macroseismic data in Italy, this study leverages these records to implement a comprehensive workflow for historical seismic source identification. This workflow consists of a pre-processing procedure and 3 different stages: (i) reconstruction of seismogenic sources; (ii) ground shaking simulations; and (iii) validation through residual analysis. In particular, a preliminary processing consists of detecting possible outliers in macroseismic intensity distributions to better constrain the reconstruction of earthquake seismogenic sources. In this study, the complete workflow is tested on three instrumental earthquakes with different characteristics to explore the overall applicability of the method. These events are the 1984 Monti della Meta (Mw 5.8), the 1989 Prealpi Vicentine (Mw 4.85), and the 2008 Parmense (Mw 5.36) earthquakes. Consequently, this approach is applied to a historical earthquake, the 3 June 1781 Cagli earthquake (Central Apennines). For this event, seismogenic sources are reconstructed from two alternative, but plausible and reliable, macroseismic fields, i.e., the intensity distribution in DBMI15 (Monachesi, 1987) and the dataset from Guidoboni et al. (2018), to quantitatively evaluate the impact of different datasets in terms of earthquake parameterisation and source geometries.

The results of this study emphasise that the proposed workflow, integrating an initial pre-processing of macroseismic fields, can be a useful tool for reconstructing seismogenic sources consistent with macroseismic data and for generating realistic shaking scenarios, especially for past events.

2 Data selection and pre-processing

In the CPTI15 catalogue, the parametrisation of historical earthquakes is performed using the Boxer code (Gasperini et al., 1999, 2010), which is applied to the macroseismic field, hereinafter referred to as the preferred dataset, provided in DBMI15. Specifically, macroseismic epicentres and magnitudes are estimated using the “Method 0” implemented in Boxer. This approach determines the epicentral location as the barycentre of the sites experiencing the highest intensities, and the magnitude is inferred as the average of the magnitude estimates, for each intensity class, computed from the area of the circular isoseismal with radius equivalent to the average epicentre-to-site distance for that intensity level. These magnitude values are calculated with the IPE by Sibol et al. (1987), which also considers epicentral intensity. The final magnitude is then obtained as a weighted trimmed mean of the independent estimates derived from all intensity classes (see Gasperini et al., 2010, for further details). This parametrisation strongly depends on the quantity and spatial distribution of the input macroseismic data. In this work, a set of 191 earthquakes was selected from CPTI15 as a test dataset, with moment magnitudes (Mw) ranging between 5.5 and 7.0, occurring in the period 1117–2017 (Fig. 1). This magnitude threshold was chosen to focus on events associated with seismogenic sources capable of generating substantial ground shaking. The events selection was based on the following criteria: (i) at least three associated IDPs, to exclude poorly constrained macroseismic fields; (ii) inland epicentres, as offshore events typically produce asymmetric intensity distributions; and (iii) events occurred in areas where the seismogenic layer is shallower than 35 km, consistent

https://doi.org/10.5194/egusphere-2026-2323
Preprint. Discussion started: 11 May 2026

with the applicability range of the adopted IPE (Gomez-Capera et al., 2024), which is calibrated for shallow crustal earthquakes. Overall, the final dataset comprises 31,656 macroseismic observations, forming the basis for the subsequent analysis.

Only a subset of 24 recent events has instrumental estimates of epicentre and magnitude, available in the CPTI15 or in ASMI; these events therefore provide a benchmark for testing the methodology (Fig. 1).

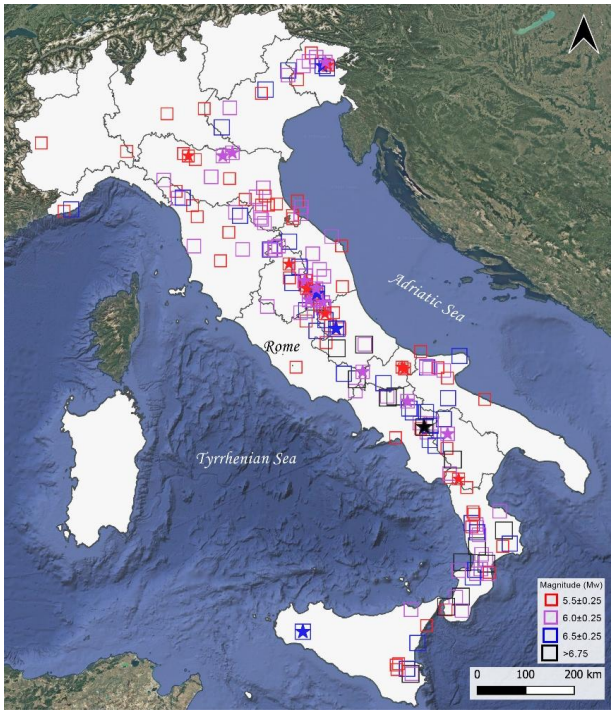

Figure 1 Selected dataset of 191 earthquakes with Mw ≥ 5.5 from the CPTI15 Catalogue (Rovida et al., 2022). Square sizes are proportional to the magnitude estimate. Starred events indicate the subset of 24 earthquakes for which instrumental solutions are available in the catalogue. Basemap source: Google Satellite imagery. Map data ©2015 Google.

Before applying the methodology, we note that the input dataset may include outliers, i.e., intensity observations that are anomalously high or low with respect to the expected attenuation pattern. To address this issue, a pre-processing step was implemented to identify and remove such outliers using the IPE proposed by Gomez-Capera et al. (2024). Intensity data exceeding three standard deviations of the model ($3\sigma \approx 2.25$ intensity units) are classified as outliers and discarded, and the resulting macroseismic dataset is considered (hereinafter referred to as the *revised* dataset). The outlier removal is necessary since the fault that best fits the data is identified through the analysis of residuals between observed and predicted intensity values (based on the median predictions of the adopted model). In this context, the presence of outliers in the macroseismic dataset may systematically bias the residual distribution and, consequently, the inferred fault geometry.

To ensure the overall consistency of our procedure, we recompute earthquake parameters of the analysed earthquake with the Boxer code, with the same settings as in CPTI15 (described in Rovida et al., 2020), starting from the revised dataset.

https://doi.org/10.5194/egusphere-2026-2323
Preprint. Discussion started: 11 May 2026

First, we tested the results of this pre-processing by computing the earthquake parameters both including and excluding the identified outliers. For the subset of 24 events with instrumental parameters, the difference between macroseismic and instrumental magnitudes is −0.12 for the preferred dataset and −0.13 for the revised dataset. Differences between macroseismic and instrumental epicentral locations are, on average, negligible.

The same analysis, performed on the full dataset of 191 earthquakes, shows that the two epicentral estimates are generally consistent, with an average difference of approximately 3 km. The comparison between magnitudes from the preferred and revised macroseismic fields shows a mean decrease of 0.15 magnitude units, within the uncertainty range of the Boxer estimates (e.g., 0.26 for pre-1900 events).
These results align with Antonucci et al. (2025), who demonstrated that randomly varying intensities in the macroseismic fields of DBMI15 by ±1 intensity degree, Boxer locations remain very stable with locations within 10 km in 83% of cases and magnitude differences within ±0.3 units in 87% of the cases.

However, significant variations in earthquake location and magnitude estimates (e.g., > 20 km and > 0.3 magnitude units) may lead to markedly different constraints on both the spatial position and the extent of the causative rupture. With this perspective, the pre-processing proves particularly effective in identifying macroseismic fields that require closer scrutiny or, in some cases, exclusion from the analysis. For completeness, Table S1 in the Supplement summarises the comprehensive details for each selected event and the results of the comparisons between solutions for the entire dataset.

The earthquakes that occurred on 25 December 1222, 4 September 1293, and 5 May 1990 show the largest epicentral shifts of approximately 20, 30, and 43 km, respectively. The 1222 and 1293 events are characterised by very few and uncertain macroseismic effects distributed over wide areas, maximum intensities documented at considerable distances from the inferred source, and large azimuthal gaps.

We consider the 1990 Potenza earthquake as a clear example of how IDPs identified as outliers can lead to a large epicentral shift (43 km). Similarly, we consider the well-documented 24 August 2016 Amatrice earthquake, characterised by well-constrained instrumental parameters and a documented seismogenic source (Tinti et al., 2016; DISS Working Group, 2025).

The May 5, 1990 Potenza earthquake struck the Southern Apennines with a Mw 5.8 from the Global Centroid Moment Tensor (GCMT, Dziewonski, 1981; http://www.globalcmt.org/CMTsearch.html). The Revised Bulletin of the International Seismological Centre (ISC 2025, www.isc.ac.uk) locates the epicentre slightly north of Potenza at [40.756°N, 15.843°E] and the Italian Seismic Bulletin (Bollettino Sismico Italiano, BSI; http://bollettinosismico.rm.ingv.it/) at [40.682°N, 15.848°E], while the CPTI15 adopts the location at [40.738°N, 15.741°E] of the previous version of the ISC Bulletin (Fig. 2c). These differences in instrumental locations, compared with more recent events, are likely due to the limited density and heterogeneous configuration of the Italian National Seismic Network at the time of the 1990 event, which was still under development and only partially digitalised. The Boxer method, applied to the macroseismic field from DBMI15 (Gasparini et al., 1991b; Fig. 2a), estimates the epicentral location and magnitude as [40.710°N, 15.299°E] and Mw 5.37, respectively. These solutions do not match any of the available instrumental locations, and for this reason it is not included in CPTI15. The pre-processing identified 116 intensity outliers within the macroseismic field (Fig. 2b). Specifically, positive residuals exceeding 3 standard deviations were concentrated in the Neapolitan area, very far from the instrumental locations, in correspondence with the highest intensity values (I = 6-7 and 7). According to Antonucci et al. (2026), these IDPs were overestimated

https://doi.org/10.5194/egusphere-2026-2323
Preprint. Discussion started: 11 May 2026

due to the cumulative damage caused by the 23 November 1980 Irpinia earthquake. Negative residuals were identified at large distances from the epicentre, particularly in southern Abruzzi, Molise, and Calabria regions. After removing these outliers, the recalculated macroseismic epicentre [40.591°N, 15.785°E] shows a significant improvement, reducing the misfit with the CPTI15-ISC2016 instrumental location from 37.3 km to only 16.7 km, relocating the epicentre near the city of Potenza (Fig. 2c). The recalculated macroseismic magnitude (Mw 5.4) is significantly lower than the instrumental one but higher than the Mw 5.19 estimated by Antonucci et al. (2026).

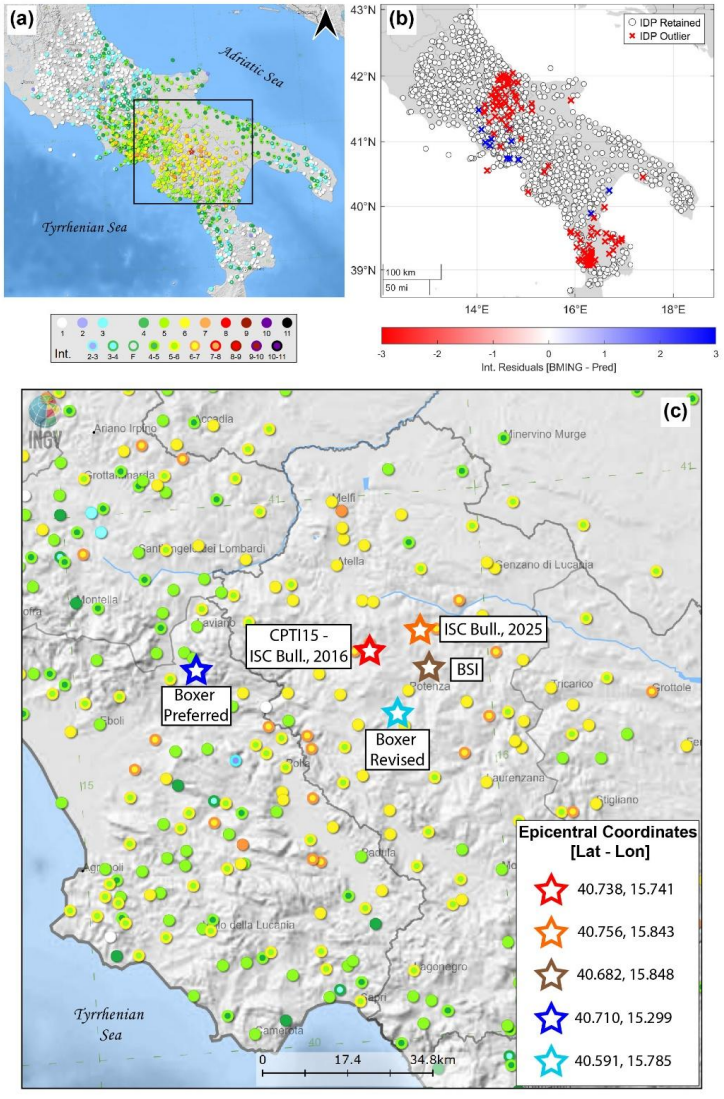

Figure 2 May 5, 1990 (Mw 5.8, GCMT) Potenza earthquake. (a) Macroseismic intensity distribution provided by DBMI15 (Locati et al., 2022) and derived from the Bollettino Macrosismico ING (BMING, Gasparini et al., 1991b). (b) Intensity residuals (blue = positive; red = negative) between BMING observations and predictions from the IPE of Gomez-Capera et al. (2024). Crosses indicate the 116 IDPs identified as outliers by the pre-processing procedure. (c) Comparison of epicentral locations: the red star represents the reference instrumental location from CPTI15 (International Seismological Centre, ISC Bulletin, 2016); the orange star indicates the updated ISC solution (ISC Bulletin, 2025); the brown star represents the instrumental location from BSI; the blue star indicates the Boxer solution derived from the preferred (BMING) macroseismic field; the light blue star represents the Boxer epicentre obtained

https://doi.org/10.5194/egusphere-2026-2323
Preprint. Discussion started: 11 May 2026

from the revised field. The map source in panels (a) and (c) is the CPTI15-DBMI15 catalogue (Locati et al., 2022; Rovida et al., 2022), which uses the NASA SRTM Digital Elevation Model (https://www.earthdata.nasa.gov/data/instruments/srtm) as background.

A second example is the August 24, 2016 Amatrice earthquake, the triggering event of the Central Italy seismic sequence. The event was located by the BSI at [42.698°N, 13.233°E]. Different moment magnitude estimates are available: Mw 6.2 from the Regional Centroid Moment Tensor (RCMT, Pondrelli, 2002) and GCMT, and Mw 6.0 from the Time Domain Moment Tensor (TDMT INGV, Scognamiglio et al., 2006, http://terremoti.ingv.it/). The adopted macroseismic field in DBMI15, derived from the field survey described in Rossi et al. (2019), consists of 221 IDPs with intensities ranging from I = 2-3 up to I ≥ 9 in the EMS-98 scale (Fig. 3a). From this macroseismic field the Boxer epicentral location and magnitude estimates are [42.683°N, 13.277°E] and Mw 6.46, as reported in CPTI15. The pre-processing identified 8 intensity outliers: two with positive residuals and six with negative ones (Fig. 3b). After removing these outliers, the recalculated macroseismic epicentre is [42.658°N, 13.288°E]. Both macroseismic epicentres are consistent with the BSI instrumental location, differing by just 3.9 km and 6 km, respectively. This slight shift is related to the removal of the IDP at Pescara del Tronto (I = 10), where the observed damage was amplified due to the location on pre-existing landslide deposits. Conversely, an improvement is observed in the magnitude estimate: the recalculated value (Mw 6.26) is notably lower and more consistent with the instrumental ones. This difference in magnitude has significant implications for the reconstruction of the seismic source, since a magnitude of Mw 6.46 would imply a rupture area of approximately 270 km², which is inconsistent with the portion of the Mt. Vettore fault system activated during the mainshock, and with structural-geological data and DInSAR modelling (~180 km²; Lavecchia et al., 2016), as well as with the observed rupture length of 20–25 km (Chiaraluce et al., 2017).

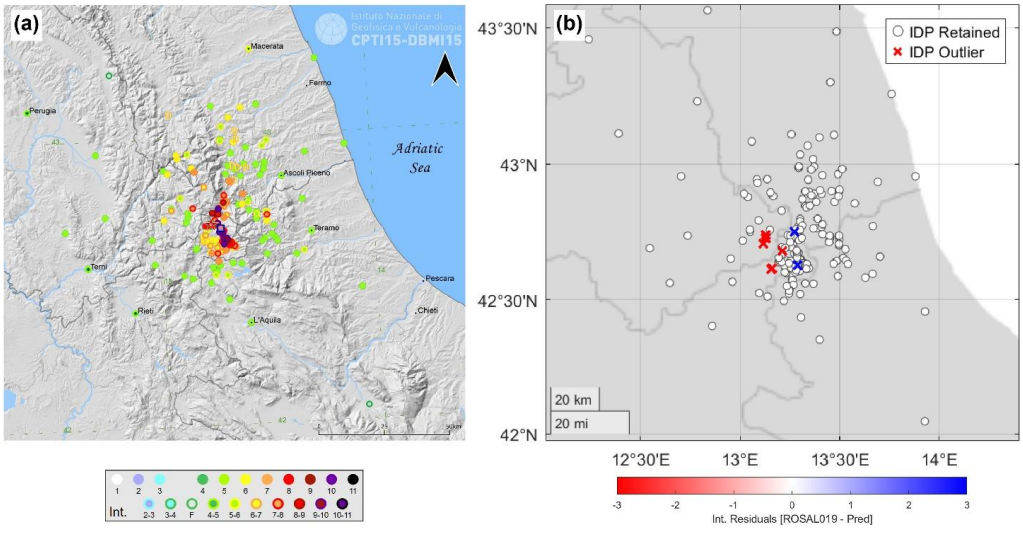

Figure 3 August 24, 2016 (Mw 6.18) Amatrice earthquake. (a) Macroseismic intensity distribution provided by DBMI15 (Locati et al., 2022) and derived from Rossi et al. (2019; ROSAL019). (b) Intensity residuals (blue = positive; red = negative) between ROSAL019 observations and values predicted from the IPE of Gomez-Capera et al. (2024). Crosses indicate the 8 IDPs identified as outliers by the pre-processing procedure and removed from the analysis. Blue crosses highlight the localities of Pescara del Tronto and Amatrice (I = 10), whereas red crosses indicate the sites of Terracino (I = 5–6), Castel S. Maria, Cittareale, Savelli, and Valcaldara (I = 5). The map source in panel (a) is the CPTI15-DBMI15 catalogue (Locati et al., 2022; Rovida et al., 2022), which uses the NASA SRTM Digital Elevation Model (https://www.earthdata.nasa.gov/data/instruments/srtm) as background.

https://doi.org/10.5194/egusphere-2026-2323
Preprint. Discussion started: 11 May 2026

3 Seismogenic source reconstruction: methodological workflow

This section describes the integrated methodological workflow for seismogenic source reconstruction, which follows the initial pre-processing step and consists of three stages, as summarised in Fig. 4. In stage 1, we estimated earthquake parameters using the Boxer code (Gasperini et al., 1999, 2010) based on the revised macroseismic fields, and in stage 2, we used these parameters to reconstruct the seismogenic sources. Fault dimensions (length and width) are calibrated according to the scaling relationships by Wells and Coppersmith (1994). In addition, for each source geometry, we defined credible parameters (e.g., strike, dip, rake, focal depth, and rupture vertices) by integrating data from several authoritative repositories: the Italian Seismic Bulletin (BSI; BSI Working Group, 2015), the Catalogue of Absolute Locations (CLASS; Latorre et al., 2022, 2023), the Engineering Strong-Motion Database (ESM; Luzi et al., 2020), the Database of Individual Seismogenic Sources (DISS; Basili et al., 2008; DISS Working Group, 2025, version 3.3.1), and the ITaly HAzard from CApable faults catalogue (ITHACA Working Group, 2019).

The 3D source geometries are modelled as rectangular planes centred on the hypocentre. We simulate ground shaking including the site effects using the ITA18 Ground Motion Model (GMM; Lanzano et al., 2019) by hypothesising variable hypocentral depths and considering the rupture distance (Rrup) as the source-to-site metrics. The resulting ground motion parameters (peak ground acceleration, PGA, and peak ground velocity, PGV), expressed in $\log_{10}$ units, are then converted into intensity values using two distinct Ground Motion to Intensity Conversion Equations (GMICEs): Gomez-Capera et al. (2020; GOM20) and Oliveti et al. (2022; OLI22).

While both equations generally align with the observed data, the OLI22 equation exhibits a saturation effect for PGV greater than 5 cm/s and PGA larger than 100 cm/s^2, which may lead to a systematic underestimation of the highest macroseismic degrees.

To identify the "best-fitting" seismogenic source (stage 3), we perform residual analyses of observed and predicted intensities (or PGA/PGV values when accelerometric recordings are available). Specifically, we compute the residuals for intensities derived from PGV, as this measure correlates most effectively with damage distribution and macroseismic intensity (Akkar and Ozen, 2005; Munafò et al., 2024; Tang et al., 2019; Gomez-Capera et al., 2020). Finally, the best-fitting source is the one that minimises the mean of the residuals (Between-Event, BE) and their root-mean-square error (RMSE). Thresholds of ±0.5 for the BE and 1 for the RMSE are identified in intensity units to consider a source as reliable.

This approach allows us to generate multiple shaking scenarios and evaluate their consistency against three key benchmarks: (i) the observed macroseismic field; (ii) recorded instrumental data (when available); and (iii) geological evidence.

https://doi.org/10.5194/egusphere-2026-2323
Preprint. Discussion started: 11 May 2026

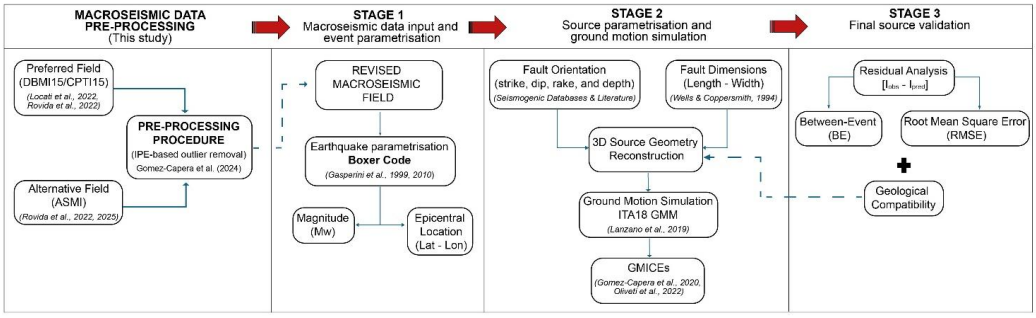

Figure 4 Schematic representation of the integrated workflow adopted for seismogenic source reconstruction, including the macroseismic data pre-processing step. The dashed blue arrows illustrate how the output of the pre-processing (i.e., the revised macroseismic field) serves as the primary input to Stage 1, and how the results from Stage 3 are used to iteratively validate and refine the 3D source geometry.

3.1 Test on instrumental events

To evaluate the effectiveness and robustness of the workflow of Fig. 4, we applied and tested it on three events characterised by instrumental metadata, chosen for their different characteristics. Specifically, the selected case studies are characterised by different magnitudes, robust macroseismic fields (> 50 IDPs), and debated or poorly constrained seismogenic sources. These events include the 1984 Monti della Meta earthquake with Mw 5.86, (https://emidius.mi.ingv.it/CPTI15-DBMI15/eq/19840511_1042_000), the 1989 Prealpi Vicentine with Mw 4.85 (https://emidius.mi.ingv.it/CPTI15-DBMI15/eq/19890913_2153_000), and the 2008 Parmense earthquakes (Mw 5.36; https://emidius.mi.ingv.it/CPTI15-DBMI15/eq/20081223_1524_000).

For the 1984 and the 2008 earthquakes, our analysis is also supported by accelerometric recordings from the Italian Accelerometric Archive (ITACA) v4.0 (Felicetta et al., 2023), which provide a further validation for the reconstructed seismogenic sources in addition to macroseismic and geologic constraints. The main features of these analysed events are summarised in Table 1.

Table 1 Summary of the selected case studies. Event ID, Event date, Time, and Epicentral Area are obtained from the CPTI15 catalogue (Rovida et al., 2022). Instrumental data indicate the availability of independent instrumental parameters (M = instrumental magnitude; H = hypocentral depth; W = accelerometric recordings). Focal mechanism indicates the fault kinematics (NF = normal fault; TF = thrust/reverse fault; SS = strike-slip fault).

Event ID	Event date	Time (UTC)	Epicentral Area	Instrumental data	Focal mechanism
19840507_1749_000	7 May 1984	17:50:--	Monti della Meta	M / H / W	NF
19890913_2153_000	13 September 1989	21:54:01	Prealpi Vicentine	M / H	SS
20081223_1524_000	23 December 2008	15:24:21	Parmense	M / H / W	TF

3.1.1 The 1984 Monti della Meta earthquake

The May 7, 1984 earthquake was the mainshock of the Abruzzo–Latium seismic sequence. The instrumental epicentral location and magnitude reported by the CPTI15 catalogue for this event are [41.665°N, 13.820°E] and Mw 5.86, based on CSTI1.1 (https://doi.org/10.13127/csti.1.1) and GCMT, respectively. CPTI15 also reports the macroseismic epicentral location and magnitude, which are [41.667°N, 14.057°E] and Mw 5.73, respectively.

https://doi.org/10.5194/egusphere-2026-2323
Preprint. Discussion started: 11 May 2026

The preferred macroseismic field in DBMI15, derived from the Catalogue of Strong Earthquakes in Italy (CFTI4med, Guidoboni et al., 2007), consists of 911 IDPs with intensities ranging from 2-3 to 8 MCS (Fig. 5a). The application of the pre-processing procedure on the preferred macroseismic field identified and removed 30 outliers, reducing the dataset to 881 IDPs. In this case, the recalculated parameters after the pre-processing remain unchanged, as the removed IDPs correspond to the lowest observed intensities. Although this event was instrumentally recorded, the hypocentral parameters reported by different seismic catalogues vary considerably. The macroseismic epicentre estimate differs by about 20 km from the instrumental locations provided by CSTI1.1, CLASS, and the Italian Seismicity Catalogue (Catalogo della Sismicità Italiana - CSI1.1; Castello et al., 2006, http://www.ingv.it/CSI/). Conversely, the estimated macroseismic magnitude (Mw 5.73) is consistent with the instrumental estimates.

To identify the best-fitting seismogenic source (i.e., the fault plane that minimises the misfit between observed and predicted intensities), we generated a set of 9 alternative sources by combining the instrumental solutions provided by CPTI15 (from CSTI1.1) and CLASS and the macroseismic location and magnitude estimate, with three different hypocentral depths: 6.58 km (CLASS), 11.20 km (CPTI15), and 20.5 km (CSI1.1), as shown in Table 2. For each configuration, we constructed a virtual box representing the 3D seismogenic source, assuming a NW–SE-oriented, W-dipping normal fault, in agreement with the literature (e.g., Westaway et al., 1989; Boncio et al., 1998).

Table 2 Instrumental earthquake parameters for the 1984 Monti della Meta earthquake, derived from CPTI15 (Rovida et al., 2022) and CLASS (Latorre et al., 2022) seismic catalogues, and macroseismic estimates obtained using Boxer (Gasperini et al., 2010). The table also reports the set of tested seismogenic sources based on the different parameter combinations.

Reference earthquake parameters	Data Type	Epicentre [Lat, Lon]	Mw	Strike/Dip/Rake (°)	Length (km)	Width (km)	Depth (km)	Tested Source
CPTI15 (Rovida et al., 2022)	Instrumental	[41.665°N, 13.820°E] CSTI1.1	5.86 GCMT	145/50/-90	10.4	7.3	6.58	META_001
							11.2	META_002
							20.5	META_003
CLASS (Latorre et al., 2022)	Instrumental	[41.713°N, 13.833°E]	5.90 GCMT	145/50/-90	10.9	7.5	6.58	META_004
							11.2	META_005
							20.5	META_006
Boxer method (Gasperini et al., 2010)	Macroseismic	[41.667°N, 14.057°E] Pref/Rev	5.73 Pref/Rev	145/50/-90	8.7	6.6	6.58	META_007
							11.2	META_008
							20.5	META_009

At this stage, the workflow consists of generating shaking scenarios for each source using the ITA18 GMM (Lanzano et al., 2019) to predict PGA and PGV. The simulated PGV values were converted into macroseismic intensity using the GOM20 and OLI22 equations. Subsequently, we compared the observed macroseismic intensities with the predicted ones by computing the mean of the residuals (Between-Event, BE) and their root-mean-square error (RMSE). Additionally, since accelerometric recordings are available for this earthquake, we also calculated the residuals between the predicted ground motion parameters (PGA and PGV, in log10 units) and the logarithm of the values recorded at stations reported in ITACA (Felicetta et al., 2023).

The results of these residual analyses are summarised in Table 3. Among the tested source configurations, the one that minimises residuals in terms of macroseismic intensities corresponds to the code META_004, that is generated using the CLASS hypocentral location and the GCMT moment magnitude and has a length of 10.9 km, and a width of 7.5 km (Table 2 and Fig. 5b). This solution is further supported by the validation performed against accelerometric recordings; specifically, we observed that the $RMSE_{LogPGA}$ of 0.33 is of the same order as the standard deviation of the ITA18 GMM (e.g., 0.336), the same occurs for BE_{LogPGA} (e.g., 0.16 in ITA18), $RMSE_{LogPGV}$ (e.g., 0.29 in ITA18), BE_{LogPGV} (e.g., 0.13 in ITA18).

https://doi.org/10.5194/egusphere-2026-2323
Preprint. Discussion started: 11 May 2026

Table 3 Results of the residual analyses for the hypothesised seismogenic sources of the 1984 Monti della Meta earthquake. For each source, the table reports the mean of the residuals (BE_I) and the root-mean-square error ($RMSE_I$) for PGV-derived macroseismic intensities using the GOM20 and OLI22 conversion equations. The table also reports the BE, calculated as the mean difference between the base-10 logarithms of observed and predicted peak ground motions, and RMSE from the validation against instrumental recordings. The asterisk indicates the best-fitting seismogenic source across the considered parameters.

Reference parameters	Source	BE_I - $RMSE_I$ (GOM20)	BE_I - $RMSE_I$ (OLI22)	BE_{LogPGA} (cm/s^2)	$RMSE_{LogPGA}$ (cm/s^2)	BE_{LogPGV} (cm/s)	$RMSE_{LogPGV}$ (cm/s)
CPTI15	META_001	0.41–0.80	0.64–0.92	-0.2	0.37	-0.08	0.34
	META_002	0.45–0.79	0.67–0.93	-0.23	0.37	-0.11	0.33
	META_003	0.55–0.83	0.76–1.00	-0.3	0.39	-0.17	0.34
	META_004 (*)	0.35–0.74	0.57–0.86	-0.19	0.33	-0.07	0.32
CLASS	META_005	0.39–0.74	0.61–0.88	-0.22	0.33	-0.09	0.32
	META_006	0.48–0.79	0.69–0.95	-0.28	0.37	-0.15	0.33
Boxer (Pref/Rev)	META_007	0.54–0.89	0.76–1.02	-0.35	0.45	-0.24	0.39
	META_008	0.58–0.88	0.8–1.04	-0.37	0.46	-0.26	0.4
	META_009	0.69–0.95	0.89–1.11	-0.43	0.5	-0.31	0.42

The source META_004 also exhibits the best overall agreement with the geological lineaments mapped in the study area, since its surface projection aligns with the Barrea–Castelnuovo fault system, as mapped in the ITHACA database of capable faults (https://sgi.isprambiente.it/ithaca/viewer/), and agrees with previous studies of the 1984 Abruzzo–Latium seismic sequence (Boncio et al., 1998; Pace et al., 2002). Among the sources derived from macroseismic parameters (Table 2), the META_007 source exhibits the lowest between-event error (BE_I = 0.54) and $RMSE_I$ (0.89). Although these values are broadly consistent with the adopted thresholds for selecting the best-fitting source, the surface projection of the META_007 fault trace shows poor consistency with the known geological structures in the area.

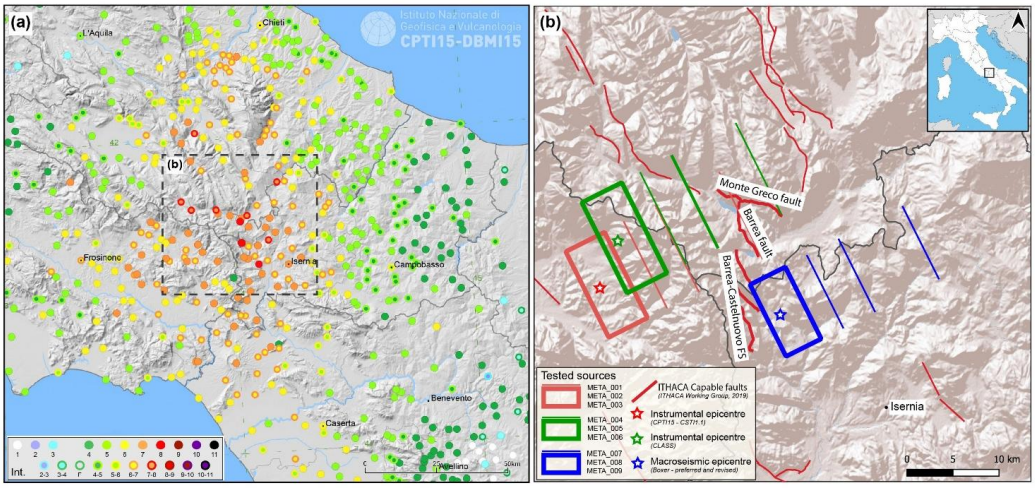

Figure 5 May 7, 1984 (Mw 5.86) Monti della Meta earthquake. (a) Macroseismic intensity distribution in DBMI15 (Locati et al., 2022) derived from CFTI4med (Guidoboni et al., 2007). (b) Comparison between tested seismogenic sources and geological constraints. Red lines indicate capable faults from the ITHACA database (ITHACA Working Group, 2019). Coloured rectangles represent the alternative source geometries explored for the 1984 Monti della Meta earthquake and their surface projections. The red and green stars represent the instrumental epicentral solutions from CPTI15 (CSTI1.1) and CLASS, respectively. The blue star indicates the macroseismic epicentres. The map source in panel (a) is the CPTI15-DBMI15 catalogue (Locati et al., 2022; Rovida et al., 2022), which uses the NASA SRTM Digital Elevation Model (https://www.earthdata.nasa.gov/data/instruments/srtm) as background. The map in panel (b) is generated using the Esri Shaded Relief basemap. Sources: Esri | Powered by Esri.

https://doi.org/10.5194/egusphere-2026-2323
Preprint. Discussion started: 11 May 2026

3.1.2 The Prealpi Vicentine earthquake

The September 13, 1989 earthquake occurred north of Schio in the Veneto region (Northern Italy). The instrumental location and magnitude provided by CPTI15 for this event are [45.882°N, 11.264°E], based on OGS-BFVG (Bollettino della Rete Sismometrica del Friuli Venezia Giulia, http://www.crs.inogs.it/bollettino/RSFVG/) and a Mw 4.85 (RCMT, Pondrelli et al., 2006b). In addition, the Boxer-derived epicentral location is [45.870°N, 11.172°E] and the Mw equal to 4.99, respectively. The adopted macroseismic field consists of 779 IDPs spread over a wide area covering the southern Alps and the Po and Veneto plains, with the light damage reported at two villages, Posina and Besenello, evaluated as intensity of 6-7 MCS (Bollettino Macrosismico ING; Gasparini et al., 1991a, Fig. 6a). The application of the pre-processing to this macroseismic field reduced the dataset to 766 IDPs. The removed outliers do not significantly affect the computation of epicentral location and magnitude. The Boxer-derived earthquake parameters remain unchanged in terms of magnitude (Mw 4.99), while the epicentral location shifts by about 4 km to [45.896°N, 11.215°E].

From a seismotectonic perspective, the 1989 earthquake was the largest instrumentally recorded event that occurred along the Schio–Vicenza Fault System (SVFS) in Northern Italy, a complex transverse structure composed of a set of NW–SE-trending and NE-dipping high-angle faults. The main fault of the SVFS is the Schio-Vicenza Lineament (SVL), a NW–SE, 120-km-long, subvertical strike-slip fault, which bounds to the east the Southern Alps (e.g., Castaldini and Panizza, 1991; Viganò et al., 2008; Vannoli et al., 2015; Zampieri et al., 2021). As reported by Vannoli et al. (2015) and Zampieri et al. (2021), the source of this event could be associated with a segment of the northern portion of the SVL. This is also supported by the focal mechanism from the RCMT (Pondrelli et al., 2006a), which indicates a right-lateral strike-slip motion with strike (146°; 56°), dip (90°; 89°), and rake (−178°; 0°). Although the scientific community generally agrees on the kinematics and the associated seismogenic source of this event, several instrumental solutions are available from different catalogues. For this reason, we tested several earthquake parametrisations to identify the source configuration that best fits the observed data and the geological fault system identified in the literature.

We generated 9 alternative seismogenic sources by considering both the instrumental solutions and the Boxer-derived macroseismic estimate. Specifically, we selected as representative solutions the instrumental locations provided by CPTI15 (from OGS) and CLASS, together with the moment magnitude (Mw 4.85) from the RCMT. For each configuration, we assumed a strike-slip fault geometry (strike = 146°, dip = 90°, rake = −179°), and three different hypocentral depths: 9 km (OGS), 12.3 km (CLASS), and 25 km to explore a deeper source (Table 4).

Table 4 Instrumental earthquake parameters for the 1989 Prealpi Vicentine earthquake, derived from CPTI15 (Rovida et al., 2022) and CLASS (Latorre et al., 2022) seismic catalogues, and macroseismic estimates obtained using Boxer (Gasperini et al., 2010). The table also reports the set of tested seismogenic sources based on the different parameter combinations.

Reference earthquake parameters	Data Type	Epicentre [Lat, Lon]	Mw	Strike/Dip/Rake (°)	Length (km)	Width (km)	Depth (km)	Tested Source
CPTI15 (Rovida et al., 2022)	Instrumental	[45.882°N, 11.264°E] OGS-BFVG	4.85 RCMT	146/90/-179	2.6	3.4	9 12.3 25	VIC_001 VIC_002 VIC_003
CLASS (Latorre et al., 2022)	Instrumental	[45.874°N, 11.134°E]	4.85 RCMT	146/90/-179	2.6	3.4	9 12.3 25	VIC_004 VIC_005 VIC_006
Boxer method (Gasperini et al., 2010)	Macroseismic	[45.896°N, 11.215°E] Rev	4.99 Rev	146/90/-179	3.2	3.8	9 12.3 25	VIC_007 VIC_008 VIC_009

https://doi.org/10.5194/egusphere-2026-2323
Preprint. Discussion started: 11 May 2026

Since no accelerometric recordings are available for this event in the ITACA database, the analysis was therefore based only on the comparison between observed and predicted macroseismic data. Sources based on the CLASS instrumental parameters (e.g., VIC_004, VIC_005, and VIC_006) exhibit the largest BE_I and $RMSE_I$ values, while the sources based on the instrumental parameters provided by the CPTI15 (i.e., OGS) provide intermediate results. In addition, an increase in BE_I and $RMSE_I$ values is observed for source geometries with hypocentral depths larger than 15 km (e.g., VIC_003, VIC_006, and VIC_012), suggesting that this event could be originated at relatively shallow depths (~ 9–12 km). The sources derived from the Boxer macroseismic estimation show generally lower BE_I and $RMSE_I$ values for both the GOM20 and OLI22 conversion equations.

Table 5 Results of the residual analysis for the hypothesised seismogenic sources of the 1989 Prealpi Vicentine earthquake. For each source, the table reports the mean of the residuals (BE_I) and the root-mean-square error ($RMSE_I$) for PGV-derived macroseismic intensities using the GOM20 and OLI22 conversion equations. The asterisk indicates the best-fitting seismogenic source across the considered parameters.

Reference parameters	Source	BE_I - $RMSE_I$ (GOM20)	BE_I - $RMSE_I$ (OLI22)
CPTI15	VIC_001	0.88–1.04	0.87–1.01
	VIC_002	0.91–1.06	0.89–1.02
	VIC_003	1.05–1.16	1.01–1.11
CLASS	VIC_004	0.90–1.05	0.90–1.02
	VIC_005	0.92–1.06	0.92–1.04
	VIC_006	1.04–1.14	1.02–1.12
Boxer (Rev)	VIC_007 (*)	0.69–0.88	0.74–0.89
	VIC_008	0.72–0.89	0.76–0.90
	VIC_009	0.87–0.99	0.89–0.99

From a geological perspective, among the tested source configurations, both the solutions based on CLASS instrumental parameters and those derived from macroseismic data are located close to the Schio–Vicenza Lineament, as mapped in the ITHACA database (Fig. 6b), which has been proposed in the literature as the potential causative structure for this event (e.g., Zampieri et al., 2021).

Although none of these sources fully satisfy the adopted selection thresholds, the lowest residuals are obtained for sources VIC_007 and VIC_008, corresponding to Boxer-derived epicentral location and magnitude with hypocentral depths of 9 km and 12.3 km, respectively (Table 5). Despite the BE_I is slightly higher than the adopted threshold ($BE_I = 0.69$) and the $RMSE_I$ is close to 1 ($RMSE_I = 0.88$), we identified the VIC_007 geometry as the best-fitting source.

https://doi.org/10.5194/egusphere-2026-2323
Preprint. Discussion started: 11 May 2026

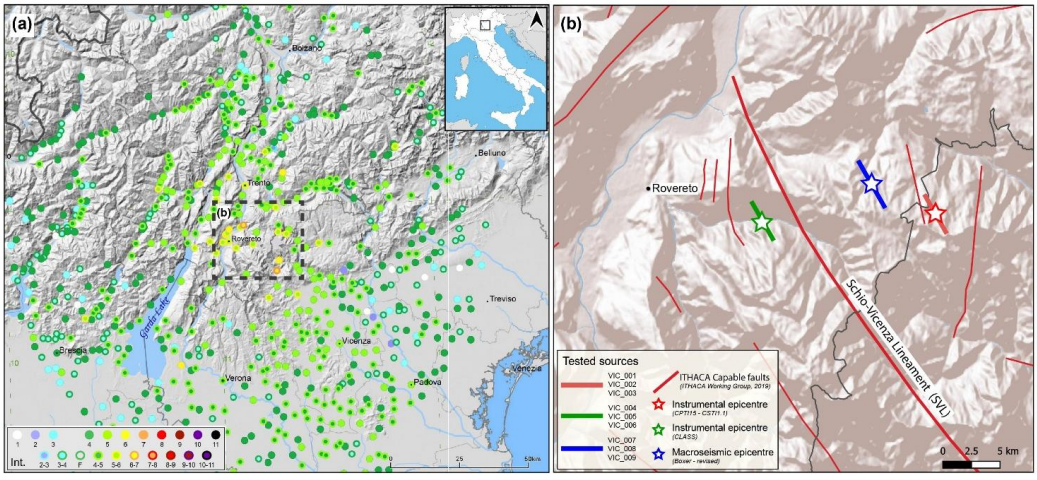

Figure 6 September 13, 1989 (Mw 4.85) Prealpi Vicentine earthquake. (a) Macroseismic intensity distribution provided by DBMI15 (Locati et al., 2022) and derived from Bollettino Macrosismico ING (BMING; Gasparini et al., 1991a). (b) Comparison between tested seismogenic sources and geological constraints. Red lines indicate capable faults from the ITHACA database (ITHACA Working Group, 2019). The tested alternative sources are represented as coloured lines, corresponding to vertical fault planes (dip = 90°), which cannot be displayed as rectangular surface projections. The red and green stars represent the adopted instrumental epicentral solutions from CPTI15 and CLASS, respectively. The blue star indicates the revised macroseismic epicentre. The map source in panel (a) is the CPTI15-DBMI15 catalogue (Locati et al., 2022; Rovida et al., 2022), which uses the NASA SRTM Digital Elevation Model (https://www.earthdata.nasa.gov/data/instruments/srtm) as background. The map in panel (b) is generated using the Esri Shaded Relief basemap. Sources: Esri | Powered by Esri.

3.1.3 The 2008 Parmense earthquake

The December 23, 2008 Parmense earthquake struck the northern Apennines between the provinces of Reggio Emilia and Parma. The instrumental location and magnitude provided by CPTI15 for this event are [44.544°N, 10.345°E], based on BSI (http://bollettinosismico.rm.ingv.it) and a Mw 5.36, based on TDMT INGV (Scognamiglio et al., 2006; https://doi.org/10.13127/TDMT), harmonised to RCMT according to Lolli et al. (2020). The macroseismic epicentre and magnitude provided by CPTI15 are [44.609°N, 10.261°E] and Mw 5.17, respectively. The adopted macroseismic field (Ercolani et al., 2009), consists of 291 IDPs with intensities ranging from 2 to 6-7 in the MCS scale (Fig. 7a). The application of the pre-processing did not modify the dataset; therefore, the Boxer-derived earthquake parameters remain unchanged.

From a seismotectonic perspective, this earthquake affected a sector of Northern Apennines characterised by compressional tectonics and by a relatively high seismicity rate. In this region, shallow earthquakes are generally located along the highest peaks of the range, while deeper events (> 10 km) occur in the outer sectors. According to BSI, the hypocentre of this event was located at a depth of about 23 km. Regarding the seismogenic source of the event, the Italian Database of Individual Seismogenic Sources (DISS) attributed it to an Individual Seismogenic Source (ISS) labelled 'ITIS135 Neviano degli Arduini'. This ISS represents a reverse structure (strike = 98°, dip = 55°, and rake = 79°) based on the focal solution from the RCMT (Pondrelli et al., 2006b).

For this event, the hypocentral parameters reported by BSI and CLASS are overall consistent in terms of location, magnitude, and depth. The instrumental locations differ by only 2 km, and the corresponding hypocentral depths are 22.9 km (BSI) and 19.6 km (CLASS). Additionally, ground motion recordings are available at 35 stations from the ITACA database (Felicetta et al., 2023). Despite this general agreement among the instrumental solutions, the application of our workflow allows us to explore which source configuration is most consistent with the available accelerometric recordings, macroseismic data, and geological constraints.

https://doi.org/10.5194/egusphere-2026-2323
Preprint. Discussion started: 11 May 2026

In this case, we generated three virtual seismogenic sources by considering the instrumental parameters provided by CPTI15 (from BSI) and CLASS, together with the macroseismic estimate (Table 6). For each source configuration, we assumed a S-dipping reverse source geometry, consistent with the ITIS135 proposed by the DISS database.

Table 6 Instrumental earthquake parameters for the 2008 Parmense earthquake, derived from CPTI15 (Rovida et al., 2022) and CLASS (Latorre et al., 2022) seismic catalogues, and macroseismic estimate obtained using Boxer (Gasperini et al., 2010). The table also reports the set of tested seismogenic sources based on the different parameter combinations.

Reference earthquake parameters	Data Type	Epicentre [Lat, Lon]	Mw	Strike/Dip/Rake (°)	Length (km)	Width (km)	Depth (km)	Tested Source
CPTI15 (Rovida et al., 2022)	Instrumental	[44.544°N, 10.345°E] BSI	5.36 TDMT	98/55/79	5.2	5	22.9	PARM_001
CLASS (Latorre et al., 2022)	Instrumental	[44.552°N, 10.366°E]	5.36 TDMT	98/55/79	5.2	5	19.6	PARM_002
Boxer method (Gasperini et al., 2010)	Macroseismic	[44.609°N, 10.261°E] Pref/Rev	5.17 Pref/Rev	98/55/79	4	4.4	22.9	PARM_003

The results of the residual analyses (Table 7) show that both PARM_001 and PARM_002 satisfy the adopted thresholds for the identification of the best-fitting source. PARM_001 is based on the CPTI15-BSI instrumental solution, whereas PARM_002 derives from the CLASS solution. Both configurations minimise the residuals for macroseismic intensities, indicating a good agreement between observed and predicted data. Consistently, the comparison between predicted ground motion parameters and recorded accelerometric data (PGA and PGV, in log10 units) shows comparable results for both source configurations. In particular, $RMSE_{LogPGV}$ and $RMSE_{LogPGA}$ values are 0.26 and 0.34, respectively, which are in line with the standard deviation of the ITA18 GMM (0.29 for PGV and 0.33 for PGA). However, PARM_001 is selected as the best-fitting seismogenic source, as it is consistent with the seismogenic source ITIS135 (Neviano degli Arduini) reported in the DISS database (Fig. 7b). In contrast, the PARM_003 source geometry, derived from macroseismic data, does not satisfy the adopted thresholds for either of the tested conversion equations ($BE_I > 0.5$ and $RMSE_I > 1$; Table 7), indicating a poorer agreement between observed and predicted intensities.

Table 7 Results of the residual analyses for the hypothesised seismogenic sources of the 2008 Parmense earthquake. For each source, the table reports the mean of the residuals (BE_I) and the root-mean-square error ($RMSE_I$) for PGV-derived macroseismic intensities using the GOM20 and OLI22 conversion equations. The table also reports the BE, calculated as the mean difference between the base-10 logarithms of observed and predicted peak ground motions, and RMSE from the validation against instrumental recordings. The asterisk indicates the best-fitting seismogenic source across the considered parameters.

Reference parameters	Source	BE_I - $RMSE_I$ (GOM20)	BE_I - $RMSE_I$ (OLI22)	BE_{LogPGA} (cm/s^2)	$RMSE_{LogPGA}$ (cm/s^2)	BE_{LogPGV} (cm/s)	$RMSE_{LogPGV}$ (cm/s)
CPTI15	PARM_001 (*)	0.53–0.78	0.64–0.80	-0.05	0.34	0.00	0.26
CLASS	PARM_002	0.45–0.76	0.54–0.75	-0.04	0.34	0.01	0.26
Boxer (Pref/Rev)	PARM_003	0.85–1.01	0.84–0.96	-0.22	0.39	-0.19	0.30

https://doi.org/10.5194/egusphere-2026-2323
Preprint. Discussion started: 11 May 2026

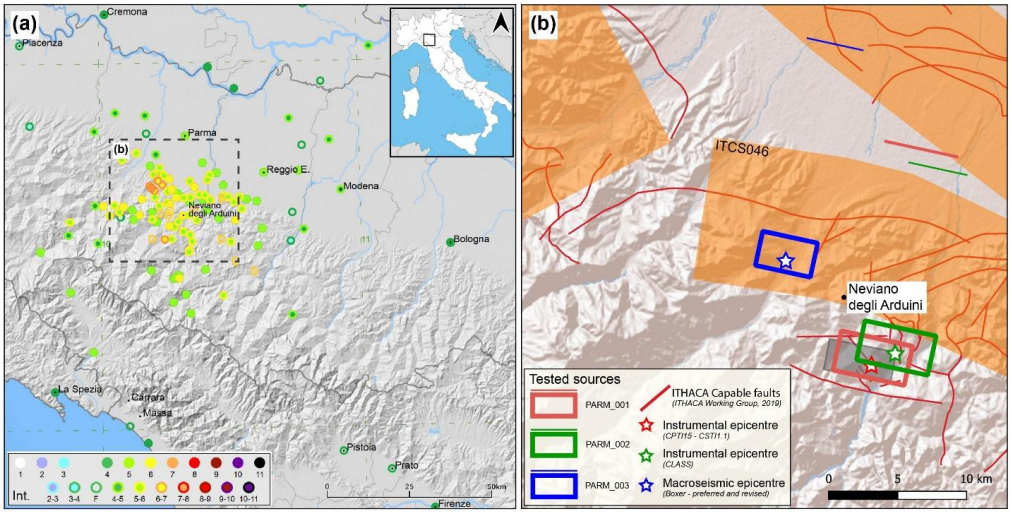

Figure 7 December 23, 2008 (Mw 5.36) Parmense earthquake. (a) Macroseismic intensity distribution in DBMI15 (Locati et al., 2022) and derived from Ercolani et al. (2009). (b) Comparison between tested seismogenic sources and geological constraints. Red lines indicate capable faults from the ITHACA database (ITHACA Working Group, 2019). Coloured rectangles represent the alternative source geometries explored for the 2008 Parmense earthquake. The orange shaded area represents the Composite Seismogenic Source (CSS) "ITCS046", while the grey rectangle indicates the proposed Individual Seismogenic Source (ISS) "ITIS135 Neviano degli Arduini", both from the DISS database (DISS Working Group, 2025). The red and green stars represent the instrumental epicentral solutions from BSI (as adopted by CPTI15) and CLASS, respectively. The blue star indicates the macroseismic epicentres. The map source in panel (a) is the CPTI15-DBMI15 catalogue (Locati et al., 2022; Rovida et al., 2022), which uses the NASA SRTM Digital Elevation Model (https://www.earthdata.nasa.gov/data/instruments/srtm) as background. The map in panel (b) is generated using the Esri Shaded Relief basemap. Sources: Esri | Powered by Esri.

3.2 Application to a historical event: The 1781 Cagli earthquake

For the application of the proposed workflow to a historical event, we selected the June 3, 1781 Cagli earthquake (https://emidius.mi.ingv.it/CPTI15-DBMI15/eq/17810603_0000_000). This earthquake was one of the largest and most damaging events that affected the Marche internal region in the last centuries.

Among the historical earthquakes included in our dataset, this event is characterised by the absence of a clear and unique seismotectonic interpretation. For this reason, it represents an appropriate case study to illustrate the application of the workflow to a historical event, i.e., where instrumental data are unavailable. In addition, it offers the opportunity to explore the influence of an alternative macroseismic field selected from those archived in the Italian Archive of Historical Earthquake Data (ASMI; Rovida et al., 2017, 2025) on the identification of the best seismogenic source.

According to CPTI15, the Boxer-derived epicentral location and magnitude of the 1781 Cagli earthquake are [43.596°N, 12.512°E] and Mw 6.51, respectively. These estimates were obtained from the macroseismic field adopted as the preferred in DBMI15. This intensity dataset (Monachesi, (1987; hereafter MONA987) consists of 157 IDPs with intensities ranging from 3-4 to 10 MCS (Fig. 8a). The alternative macroseismic field considered in this analysis was compiled by Guidoboni et al. (2018), hereafter CFTI5med. This dataset presents a slightly different spatial distribution of intensities and consists of 151 IDPs, ranging from 2-3 to 10 MCS (Fig. 8c). The macroseismic epicentre calculated from this dataset at [43.576°N, 12.548°E] results shifted to 3.6 km SE with respect to that from MONA987, and the corresponding magnitude estimate is Mw 6.33. The application of the pre-processing on both the preferred and the alternative macroseismic field do not affect the macroseismic parameters.

https://doi.org/10.5194/egusphere-2026-2323
Preprint. Discussion started: 11 May 2026

From a geological perspective, the 1781 Cagli earthquake is located between the northern Apennine fold-and-thrust belt and the Umbria-Marche ridge, in a zone currently undergoing crustal extension. However, according to the literature, outcropping active faults capable of producing an event such as the 1781 earthquake are not mapped in this sector of the Apennines.

Despite the absence of documented capable faults or clear geological evidence, the DISS database suggests that the causative source of the 1781 Cagli earthquake is located on the Montiego thrust, a segment of a major thrust reactivated under the current extensional regime and emerging along the Adriatic coastline. Based on this interpretation and the macroseismic parameters proposed by CPTI15, the event is associated with the ISS labelled "ITIS047 Cagli". This ISS represents a SW-dipping structure (strike = 134°, dip = 30°, and rake = -90°), with the strike consistent with the general orientation of the frontal thrusts of the Apennines in this sector, while the rake reflects regional geodynamic considerations. Conversely, De Donatis et al. (2020) documented the presence of a fault system in the Monte Nerone area. Specifically, this NW–SE to WNW–ESE striking system of shallow normal faults, including the Sassorotto and Col Lungo faults, shows stratigraphic, structural, and geomorphological evidence of extensional tectonics, and they suggested that this fault system may be capable of generating large earthquakes, as the 1781 Cagli event.

To identify the best seismogenic source for this event, we applied the proposed workflow considering both the seismotectonic interpretations described above and the two alternative macroseismic fields. Specifically, we generated four alternative source configurations (Table 8): two (CAGLI_001 and CAGLI_003) consistent with the orientation of the DISS hypothesis (ITIS047 Cagli) and two (CAGLI_002 and CAGLI_004) consistent with the orientation of the fault system described by De Donatis et al. (2020). For the latter two source hypotheses, we assumed a normal fault (strike = 110°, dip = 55°, and rake = −90°). Each virtual source was constructed around the hypocentre, with rupture length and width derived from the magnitude estimates using Wells and Coppersmith (1994). The location and the dimensions of CAGLI_001 and CAGLI_002 are derived from the parameters obtained with the MONA987 intensity dataset, those of CAGLI_003 and CAGLI_004 with the macroseismic field from CFTI5med. For all source configurations, a fixed hypocentral depth of 10 km was assumed, consistent with the average depth of earthquakes in the area.

Table 8 Sources tested for the 1781 Cagli earthquake. Source geometries (Strike, Dip, Rake) for CAGLI_001 and CAGLI_003 are based on the ITIS047 Cagli (Diss Working Group, 2025), whereas CAGLI_002 and CAGLI_004 are based on the orientation of the Mt. Nerone fault system (De Donatis et al., 2020).

Reference earthquake parameters	Epicentre [Lat, Lon]	Mw	Strike/Dip/Rake (°)	Length (km)	Width (km)	Depth (km)	Tested Source
MONA987 (Monachesi, 1987)	[43.596°N, 12.512°E]	6.51	134/30/-90	24.8	11.7	10	CAGLI_001
MONA987 (Monachesi, 1987)	[43.596°N, 12.512°E]	6.51	110/55/-90	24.8	11.7	10	CAGLI_002
CFTI5med (Guidoboni et al., 2018)	[43.576°N, 12.548°E]	6.33	134/30/-90	10.1	10.1	10	CAGLI_003
CFTI5med (Guidoboni et al., 2018)	[43.576°N, 12.548°E]	6.33	110/55/-90	10.1	10.1	10	CAGLI_004

The results of the analysis are summarised in Table 9. The residuals obtained with the GOM20 model exhibit negative BE_I values for all tested source configurations, indicating a general overestimation of the observed intensities. In contrast, the residuals obtained with OLI22 indicate overestimation for the CAGLI_001 and CAGLI_002 sources (Fig. 8b), and underestimation for CAGLI_003 and CAGLI_004 (Fig. 8d); nevertheless, they are significantly lower than those obtained with GOM20.

Table 9 Results of the residual analysis for the tested seismogenic sources of the 1781 Cagli historical earthquake. For each source, the table reports the mean of the residuals (BE_I) and the root-mean-square error ($RMSE_I$) for PGV-derived macroseismic intensities using the GOM20 and OLI22 conversion equations.

https://doi.org/10.5194/egusphere-2026-2323
Preprint. Discussion started: 11 May 2026

Test macroseismic field	Source	BE_I - $RMSE_I$ (GOM20)	BE_I - $RMSE_I$ (OLI22)
MONA987	CAGLI_001	-0.71–1.22	-0.02–0.94
MONA987	CAGLI_002	-0.91–1.37	-0.17–0.97
CFTI5med	CAGLI_003	-0.37–1.01	0.23–0.97
CFTI5med	CAGLI_004	-0.56–1.10	0.06–0.90

Overall, the lowest BE_I and $RMSE_I$ values, for both the GOM20 and OLI22 conversion equations, are obtained for the CAGLI_003 and CAGLI_004 source configurations (Fig. 8d). Although the strike orientation of CAGLI_003, consistent with the DISS source (ITIS047), is more compatible with the regional structural setting, both configurations provide a comparable fit to the observed macroseismic data. In particular, the predicted intensities derived from these fault models exhibit smaller residuals irrespective of the adopted GMICE. The comparison between the two macroseismic datasets indicates that the CFTI5med dataset (Guidoboni et al., 2018) systematically yields lower residuals than the MONA987 dataset (Monachesi, 1987), suggesting that a lower magnitude (Mw 6.33) may be more consistent with this event.

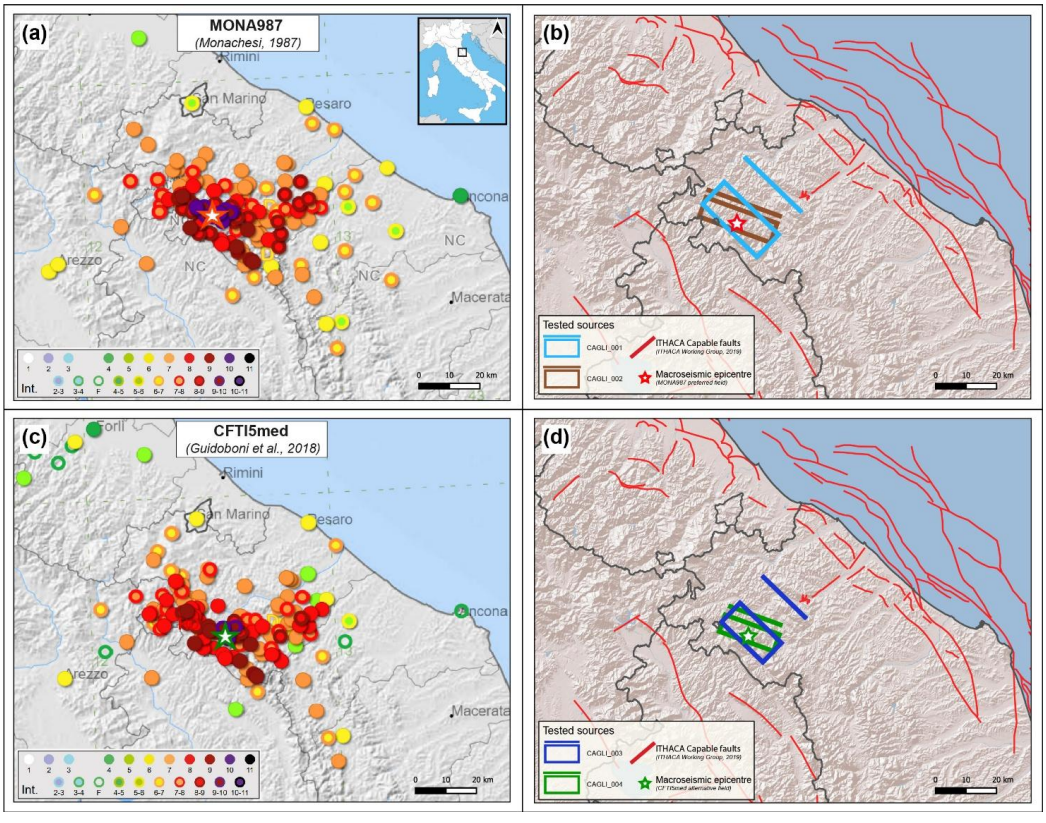

Figure 8 (a) Macroseismic intensity distribution from the MONA987 dataset (Monachesi, 1987). (b) Tested source configurations (CAGLI_001 and CAGLI_002). (c) Macroseismic intensity distribution from the CFTI5med dataset (Guidoboni et al., 2018). (d) Tested source configurations (CAGLI_003 and CAGLI_004). Red lines represent capable faults from the ITHACA database (ITHACA Working Group, 2019), while red and green stars indicate the macroseismic epicentres derived from MONA987 and CFTI5med datasets, respectively. The map source in panel (a) and (c) is the CPTI15-DBMI15 catalogue (Locati et al., 2022; Rovida et al., 2022), which uses the NASA SRTM Digital Elevation Model (https://www.earthdata.nasa.gov/data/instruments/srtm) as background. The maps in panels (b) and (d) are generated using the Esri Shaded Relief basemap. Sources: Esri | Powered by Esri.

https://doi.org/10.5194/egusphere-2026-2323
Preprint. Discussion started: 11 May 2026

4. Discussion and conclusions

This study presents a comprehensive methodological workflow for identifying the seismic sources of historical earthquakes. The approach integrates an initial pre-processing stage for the identification and removal of potential outliers, followed by three main stages: (i) earthquake parameter estimation using the Boxer code, (ii) seismogenic source reconstruction and ground-motion simulation, and (iii) validation of the inferred source geometries through residual analysis (see Sect. 3) and check with geologic lineaments.

The pre-processing procedure aims at identifying macroseismic fields that require closer scrutiny or, in some cases, exclusion from the analysis. Although the presence of some possible over- or underestimated intensity value does not significantly change the macroseismic location and magnitude obtained with the adopted Boxer method, it may significantly affect the analysis of the residuals and, consequently, the interpretation of the geometry and dimensions of the seismogenic source.

The application of the proposed workflow to the selected instrumental earthquakes shows that macroseismic-derived parameters can provide realistic seismogenic source geometries that are mostly consistent with those derived from instrumental solutions. The validation has been performed for a wide magnitude range and with the aid of accelerometric recordings and mapped geological structures (e.g., 1984 Monti della Meta, 1989 Prealpi Vicentine, and 2008 Parmense earthquakes). The reliability of these results is confirmed by the fact that the residual values (BE and RMSE) obtained from accelerometric data align closely with the standard deviation (σ) of the adopted ITA18 GMM by Lanzano et al. (2019).

The application of the proposed workflow to the 1781 Cagli earthquake allows to select between alternative macroseismic fields for discriminating the best-fitting seismogenic source. Two alternative and reliable intensity datasets (Monachesi, 1987; Guidoboni et al., 2018) were simulated with four source hypotheses. The comparison of the residuals obtained from the simulations of the two datasets indicates that the seismogenic sources based on parameters derived from the CFTI5med dataset provide a better fit to the observed data in terms of BE_I and $RMSE_I$ values.

The results further suggest that shaking scenarios simulated with a lower magnitude estimate (i.e., Mw 6.33) could be more consistent with this event. This implies that the coherence between intensity data points (IDPs), earthquake parameters, source geometry, and ground motion simulations can lead to a more comprehensive reconstruction of both the earthquake effects and the causative fault.

Based on the findings of this study, the workflow can be systematically applied to reconstruct the seismogenic sources of the strongest Italian historical earthquakes (Mw ≥ 5.5) reported in CPTI15-DBMI15, and for which consistent intensity distributions are available.

Data availability

The data used in this study are publicly available. The selected dataset and the reference macroseismic earthquake parameters are obtained from the Catalogo Parametrico dei Terremoti Italiani (CPTI15, version 4.0; Rovida et al., 2022; https://emidius.mi.ingv.it/CPTI15-DBMI15/). The macroseismic data are retrieved from the Italian Macroseismic Database (DBMI15, version 4.0; Locati et al., 2022) and the Italian Archive of Historical Earthquake Data (ASMI; Rovida et al., 2017, 2025; https://emidius.mi.ingv.it/ASMI/). Instrumental earthquake parameters are obtained from both CPTI15 v4.0 and CLASS (Catalogue of Absolute Locations; Latorre et al., 2022; https://ingv.github.io/class/locations/). The DEM used in figures provided by the CPTI15-

https://doi.org/10.5194/egusphere-2026-2323
Preprint. Discussion started: 11 May 2026

DBMI15 catalogue is the NASA SRTM (Shuttle Radar Topography Mission), accessible at https://www.earthdata.nasa.gov/data/instruments/srtm. Other basemaps used in the figures include Google Satellite imagery (map data ©2015 Google) and Esri Shaded Relief basemaps (Sources: Esri | Powered by Esri). The revised macroseismic earthquake parameters, the epicentral distances (in km), and the magnitude differences between preferred and revised macroseismic estimates, as well as between macroseismic and instrumental solutions (when available), are reported in Table S1.

Author contributions

VG and LL conceptualized the study. VG developed the methodology, performed the analysis, and wrote the manuscript. LL, AA, and AR contributed to the interpretation of the results and critically revised the manuscript. All authors reviewed and approved the final version of the manuscript.

Competing interests

The authors declare that they have no conflict of interest.

Disclaimer

Publisher's note: Copernicus Publications remains neutral with regard to jurisdictional claims made in the text, published maps, institutional affiliations, or any other geographical representation in this paper.

Financial support

The authors declare that this research was partially funded by the Consortium REDI (REducing risks of natural DIsasters).

References

Allen, T. I., Wald, D. J., Hotovec, A. J., Lin, K.-W., Earle, P. S., and Marano, K. D.: An atlas of ShakeMaps for selected global earthquakes, Open-File Report (No. 2008-1236), U.S. Geological Survey, https://doi.org/10.3133/ofr20081236, 2008.

Antonucci, A., Augliera, P., Locati, M., and Rovida, A.: Impact of the intensity assessment on the macroseismic parameters of earthquakes in Italy, Geophysical Journal International, 242, ggaf224, https://doi.org/10.1093/gji/ggaf224, 2025.

Antonucci, A., Castellano, C., Cucci, L., and Tertulliani, A.: A thorough review of the 5 May 1990 Potenza (Southern Italy) earthquake: constraints from macroseismology and insights from hydrology, Nat. Hazards Earth Syst. Sci., 26, 1105–1118, https://doi.org/10.5194/nhess-26-1105-2026, 2026.

Akkar, S. and Özen, Ö.: Effect of peak ground velocity on deformation demands for SDOF systems, Earthquake Engng Struct. Dyn., 34, 1551–1571, https://doi.org/10.1002/eqe.492, 2005.

Basili, R., Valensise, G., Vannoli, P., Burrato, P., Fracassi, U., Mariano, S., Tiberti, M. M., and Boschi, E.: The Database of Individual Seismogenic Sources (DISS), version 3: Summarizing 20 years of research on Italy's earthquake geology, Tectonophysics, 453, 20–43, https://doi.org/10.1016/j.tecto.2007.04.014, 2008.

Bindi, D., Parolai, S., Oth, A., Abdrakhmatov, K., Muraliev, A., and Zschau, J.: Intensity prediction equations for Central Asia, Geophys. J. Int., 187, 327–337, https://doi.org/10.1111/j.1365-246X.2011.05142.x, 2011.

https://doi.org/10.5194/egusphere-2026-2323
Preprint. Discussion started: 11 May 2026

Boncio, P., Brozzetti, F., Di Matteo, P., Lavecchia, G., and Pace, B.: Il controllo dell'interazione fra strutture sincinematiche a diversa orientazione nella genesi ed evoluzione dei processi sismogenetici: l'esempio della Val di Sangro (Abruzzo), Atti del 17 Convegno G. N. G. T. S., GNGTS, 1-7, 1998.

Castaldini, D. and Panizza, M.: Inventario delle faglie attive tra i Fiumi Po e Piave e il Lago di Como (Italia Settentrionale), Il Quaternario, 4, 333–410, 1991.

Castello, B., Selvaggi, G., Chiarabba, C., and Amato, A.: Catalogo della sismicità italiana (CSI) 1981-2002, Istituto Nazionale di Geofisica e Vulcanologia (INGV) [data set], https://doi.org/10.13127/CSI.1.1, 2006.

Chiaraluce, L., Di Stefano, R., Tinti, E., Scognamiglio, L., Michele, M., Casarotti, E., Cattaneo, M., De Gori, P., Chiarabba, C., and Monachesi, G.: The 2016 central Italy seismic sequence: A first look at the mainshocks, aftershocks, and source models, Seismol. Res. Lett., 88, 757–771, https://doi.org/10.1785/0220160221, 2017.

De Donatis, M., Alberti, M., Cipicchia, M., Guerrero, N. M., Pappafico, G. F., and Susini, S.: Workflow of Digital Field Mapping and Drone-Aided Survey for the Identification and Characterization of Capable Faults: The Case of a Normal Fault System in the Monte Nerone Area (Northern Apennines, Italy), ISPRS International Journal of Geo-Information, 9, 616, https://doi.org/10.3390/ijgi9110616, 2020.

Dziewonski, A. M. and Anderson, D. L.: Preliminary reference Earth model, Phys. Earth Planet. Inter., 25, 297–356, https://doi.org/10.1016/0031-9201(81)90046-7, 1981.

DISS Working Group: Database of Individual Seismogenic Sources (DISS), Version 3.3.1: A compilation of potential sources for earthquakes larger than M 5.5 in Italy and surrounding areas. Istituto Nazionale di Geofisica e Vulcanologia (INGV) [data set], https://doi.org/10.13127/diss3.3.1, 2025.

Ercolani E., Rossi A., Vecchi M., Leschiutta I., Bernardini F., Del Mese S., Camassi R., Pondrelli S., and Tertulliani A.: Rilievo macrosismico del terremoto emiliano del 23 dicembre 2008. Quad. Geofis., 71, Istituto Nazionale di Geofisica e Vulcanologia (INGV), Roma, 41 pp., https://emidius.mi.ingv.it/ASMI/study/ERCAL009 (last access: 21April 2026), 2009.

Faenza, L., Pierdominici, S., Camassi, R., Michelini, A., Ercolani, E., and Lauciani, V.: The shakemap atlas for the city of naples, Italy, Seismol. Res. Lett., 84, 963–972, https://doi.org/10.1785/0220130048, 2013.

Felicetta, C., Russo, E., D'Amico, M. C., Sgobba, S., Lanzano, G., Mascandola, C., Pacor, F., and Luzi, L.: ITalian ACcelerometric Archive (ITACA), version 4.0, https://itaca.mi.ingv.it/ItacaNet_40/ (last access: 21 April 2026), 2023.

Gasparini, C., Tertulliani, A., Riguzzi, F., Anzidei, M., Maramai, A., Murru, M., De Rubeis, V., Vecchi, M., Del Mese, S., Vannucci, C., Conte, S., Massucci, A., and Saraceni, A. M.: Bollettino macrosismico 1989, Istituto Nazionale di Geofisica, Roma, 163 pp., https://emidius.mi.ingv.it/ASMI/study/BMING991a (last access: 21 April 2026), 1991a.

Gasparini, C., Tertulliani, A., Riguzzi, F., Anzidei, M., Maramai, A., Murru, M., De Rubeis, V., Vecchi, M., Del Mese, S., Vannucci, C., Conte, S., Massucci, A., and Saraceni, A. M.: Bollettino macrosismico 1990, Istituto Nazionale di Geofisica, Roma, 210 pp., https://emidius.mi.ingv.it/ASMI/study/BMING991b (last access: 21 April 2026), 1991b.

https://doi.org/10.5194/egusphere-2026-2323
Preprint. Discussion started: 11 May 2026

Gasperini, P., Bernardini, F., Valensise, G., and Boschi, E.: Defining seismogenic sources from historical earthquake felt reports, Bull. Seismol. Soc. Am., 89, 94–110, 1999

Gasperini, P., Vannucci, G., Tripone, D., and Boschi, E.: The Location and Sizing of Historical Earthquakes Using the Attenuation of Macroseismic Intensity with Distance, Bull. Seismol. Soc. Am., 100, 2035–2066, https://doi.org/10.1785/0120090330, 2010.

Gironelli, V., Volatili, T., Luzi, L., Brunelli, G., Zambrano, M., and Tondi, E.: Ground motion simulations of historical earthquakes: the case study of the Fabriano (1741, Mw = 6.1) and Camerino (1799, Mw = 6.1) earthquakes in central Italy, Bull. Earthq. Eng., 21, 5809–5830, https://doi.org/10.1007/s10518-023-01759-y, 2023.

Global Centroid Moment Tensor Project, http://www.globalcmt.org (last access: 21 April 2026)

Gomez-Capera, A. A., D'Amico, M., Lanzano, G., Locati, M., and Santulin, M.: Relationships between ground motion parameters and macroseismic intensity for Italy, Bull. Earthq. Eng., 18, 5143–5164, 2020.

Gomez-Capera, A. A., Santulin, M., D'Amico, M., D'Amico, V., Locati, M., Meletti, C., and Varini, E.: Macroseismic intensity attenuation models calibrated in Mw for Italy, Bull. Earthq. Eng., 22(3), 795-843, https://doi.org/10.1007/s10518-020-00905-0, 2024.

Gruppo di Lavoro CSTI: Catalogo Strumentale dei Terremoti Italiani dal 1981 al 1996 (Versione 1.1), Istituto Nazionale di Geofisica e Vulcanologia (INGV), https://doi.org/10.13127/csti.1.1, 2005.

Grünthal, G. (Ed.): European Macroseismic Scale 1998, Vol. 13, Conseil de l'Europe, Cahiers du Centre Européen de Géodynamique et de Séismologie, Luxembourg, 99 pp., ISBN N2-87977-008-4, 1998.

Guidoboni, E., Ferrari, G., Mariotti, D., Comastri, A., Tarabusi, G., and Valensise G.: CFTI4Med, Catalogue of Strong Earthquakes in Italy (461 B.C.-1997) and Mediterranean Area (760 B.C.-1500), INGV-SGA, http://storing.ingv.it/cfti4med, 2007.

Guidoboni, E., Ferrari, G., Mariotti, D., Comastri, A., Tarabusi, G., Sgattoni, G., and Valensise, G.: CFTI5Med, Catalogo dei Forti Terremoti in Italia (461 a.C.-1997) e nell'area Mediterranea (760 a.C.-1500), Istituto Nazionale di Geofisica e Vulcanologia (INGV) [data set], https://doi.org/10.6092/INGV.IT-CFTI5, 2018.

Istituto Nazionale di Oceanografia e di Geofisica Sperimentale - Centro di Ricerche Sismologiche. Bollettino della Rete Sismometrica del Friuli Venezia Giulia. http://www.crs.inogs.it/bollettino/RSFVG, (last access: 21 April 2026).

BSI Working Group: Bollettino Sismico Italiano (BSI), Istituto Nazionale di Geofisica e Vulcanologia (INGV), https://doi.org/10.13127/bsi, 2015.

International Seismological Centre: On-line Bulletin, https://doi.org/10.31905/D808B830, 2025.

ITHACA (ITaly HAzard from CApable faulting): A database of active capable faults of the Italian territory, Version December 2019, ISPRA Geological Survey of Italy, http://sgi2.isprambiente.it/ithacaweb/Mappatura.aspx, (last access: 21 April 2026).

Lanzano, G., Luzi, L., Pacor, F., Felicetta, C., Puglia, R., Sgobba, S., and D'Amico, M.: A revised ground-motion prediction model for shallow crustal earthquakes in Italy, Bulletin of the Seismological Society of America, 109, 525–540, https://doi.org/10.1785/0120180210, 2019.

https://doi.org/10.5194/egusphere-2026-2323
Preprint. Discussion started: 11 May 2026

Lavecchia, G., Castaldo, R., Nardis, R. de, Novellis, V. D., Ferrarini, F., Pepe, S., Brozzetti, F., Solaro, G., Cirillo, D., Bonano, M., Boncio, P., Casu, F., Luca, C. D., Lanari, R., Manunta, M., Manzo, M., Pepe, A., Zinno, I., and Tizzani, P.: Ground deformation and source geometry of the 24 August 2016 Amatrice earthquake (Central Italy) investigated through analytical and numerical modeling of DInSAR measurements and structural-geological data, Geophysical Research Letters, 43, 12,389-12,398, https://doi.org/10.1002/2016GL071723, 2016.

Latorre D., Di Stefano R., Castello B., Michele M., and Chiaraluce L.: Catalogo delle Localizzazioni ASSolute (CLASS): locations (Version 1) [Data set], Istituto Nazionale di Geofisica e Vulcanologia (INGV), https://doi.org/10.13127/class.1.0, 2022.

Latorre D., Di Stefano R., Castello B., Michele M., and Chiaraluce L.: An updated view of the Italian seismicity from probabilistic location in 3D velocity models: The 1981–2018 Italian catalog of absolute earthquake locations (CLASS), Tectonophysics, 846, 229664, https://doi.org/10.1016/j.tecto.2022.229664, 2023.

Locati, M., Camassi, R., Rovida, A., Ercolani, E., Bernardini, F., Castelli, V., Caracciolo, C. H., Tertulliani, A., Rossi, A., Azzaro, R., D'Amico, S., and Antonucci, A.: Database Macrosismico Italiano DBMI15, versione 4.0, INGV [data set], https://doi.org/10.13127/DBMI/DBMI15.4, 2022.

Lolli, B., Randazzo, D., Vannucci, G., and Gasperini, P.: The homogenized instrumental seismic catalog (HORUS) of Italy from 1960 to present, Seismological Society of America, 91, 3208–3222, https://doi.org/10.1785/0220200148, 2020.

Lolli, B., Gasperini, P., and Vannucci, G.: Recalibration of the intensity prediction equation in Italy using the macroseismic dataset DBMI15 version 2.0. Seismol. Res. Lett., 95(4), 2399-2408, https://doi.org/10.1785/0220230212, 2024.

Luzi, L., Lanzano, G., Felicetta, C., D'Amico, M. C., Russo, E., Sgobba, S., Pacor, F., and ORFEUS Working Group: Engineering Strong Motion Database (ESM) (Version 2.0), https://doi.org/10.13127/ESM.2, 2020.

Medvedev, S., Sponheuer, W., and Karník, V.: Neue seismische Skala Intensity scale of earthquakes, in: 7. Tagung der Europäischen Seismologischen Kommission vom 24.9. bis 30.9.1962, in Jena, Veröff. Institut für Bodendynamik und Erdbebenforschung in Jena, Deutsche Akademie der Wissenschaften zu Berlin, 77, 69–76, 1964.

Monachesi, G. (Ed.): Revisione della sismicità di riferimento per i comuni di Cerreto d'Esi (AN), Esanatoglia (MC), Serra San Quirico (AN), Osservatorio Geofisico Sperimentale, Macerata, Internal report, 240 pp., 1987.

Munafò, I., Akinci, A., Taroni, M., Faenza, L., Oliveti, I., Antonucci, A., Gomez-Capera, A. A., and Rovida, A.: Studying past earthquakes with modern techniques: Ground-motion simulations for the 11 January 1693 Noto earthquake in Italy, Seismol. Res. Lett., 95, 3387–3405, https://doi.org/10.1785/%25200220240105, 2024.

Oliveti, I., Faenza, L., and Michelini, A.: New reversible relationships between ground motion parameters and macroseismic intensity for Italy and their application in ShakeMap, Geophys. J. Int., 231, 1117–1137, https://doi.org/10.1093/gji/ggac245, 2022.

Oliveti, I., Faenza, L., Antonucci, A., Locati, M., Rovida, A., and Michelini, A.: The ShakeMap atlas of historical earthquakes in Italy: Configuration and Validation, Seismol. Res. Lett., 95, 21–37, https://doi.org/10.1785/0220230138, 2024.

https://doi.org/10.5194/egusphere-2026-2323
Preprint. Discussion started: 11 May 2026

737 Pace, B., Boncio, P., and Lavecchia, G.: The 1984 Abruzzo earthquake (Italy): an example of
738 seismogenic process controlled by interaction between differently oriented synkinematic faults,
739 Tectonophysics, 350, 237–254, https://doi.org/10.1016/S0040-1951(02)00118-X, 2002.

740 Pasolini, C., Albarello, D., Gasperini, P., D'Amico, V., and Lolli, B.: The Attenuation of Seismic
741 Intensity in Italy, Part II: Modeling and Validation, B. Seismol. Soc. Am., 98, 692–708,
742 https://doi.org/10.1785/0120070021, 2008.

743 Pettenati, F., Sirovich, L., and Cavallini, F.: Objective treatment and synthesis of macroseismic
744 intensity data sets using tessellation, Bull. Seismol. Soc. Am., 89, 1203–1213, 1999.

745 Pondrelli, S., Salimbeni, S., Ekström, G., Morelli, A., Gasperini P., and Vannucci, G.: The Italian
746 CMT dataset from 1977 to the present, Phys. Earth Planet. In., 159, 286–303,
747 https://doi.org/10.1016/j.pepi.2006.07.008, 2006.

748 Pondrelli, S. and Salimbeni, S.: Italian CMT Dataset [Data set], Istituto Nazionale di Geofisica e
749 Vulcanologia (INGV), https://doi.org/10.13127/rcmt/italy, 2006.

750 Provost, L. and Scotti, O.: QUake-MD: Open-Source Code to Quantify Uncertainties in Magnitude–
751 Depth Estimates of Earthquakes from Macroseismic Intensities, Seismol. Res. Lett., 91, 2520–2530,
752 https://doi.org/10.1785/0220200064, 2020.

753 Rossi, A., Tertulliani, A., Azzaro, R., Graziani, L., Rovida, A., Maramai, A., Pessina, V.,
754 Hailemikael, S., Buffarini, G., Bernardini, F., Camassi, R., Del Mese, S., Ercolani, E., Fodarella, A.,
755 Locati, M., Martini, G., Paciello, A., Paolini, S., Arcoraci, L., Castellano, C., Verrubbi, V., and
756 Stucchi, M.: The 2016–2017 earthquake sequence in Central Italy: macroseismic survey and damage
757 scenario through the EMS-98 intensity assessment, Bull. Earthq. Eng., 17, 2407–2431,
758 https://doi.org/10.1007/s10518-019-00556-w, 2019.

759 Rovida, A., Locati, M., Antonucci, A., and Camassi, R. (Eds.): Archivio Storico Macrosismico
760 Italiano (ASMI), Istituto Nazionale di Geofisica e Vulcanologia (INGV),
761 https://doi.org/10.13127/asmi, 2017.

762 Rovida, A., Locati, M., Camassi, R., Lolli, B., and Gasperini, P.: The Italian earthquake catalogue
763 CPTI15, B. Earthq. Eng, 18, 2953–2984, https://doi.org/10.1007/s10518-020-00818-y, 2020.

764 Rovida, A., Locati, M., Camassi, R., Lolli, B., Gasperini, P., and Antonucci, A.: Catalogo Parametrico
765 dei Terremoti Italiani (CPTI15), versione 4.0, Istituto Nazionale di Geofisica e Vulcanologia (INGV)
766 [data set], https://doi.org/10.13127/CPTI/CPTI15.4, 2022

767 Rovida, A., Locati, M., Antonucci, A., and Camassi, R.: The Italian Archive of Historical Earthquake
768 Data, ASMI, Earth Syst. Sci. Data, 17, 3109–3124, https://doi.org/10.5194/essd-17-3109-2025, 2025.

769 Rotondi, R., Varini, E., and Brambilla, C.: Probabilistic modelling of macroseismic attenuation and
770 forecast of damage scenarios, Bull. Earthq. Eng., 14, 1777–1796, https://doi.org/10.1007/s10518-
771 015-9781-7, 2016.

772 Sbarra, P., Burrato, P., Tosi, P., Vannoli, P., e Rubeis, V., and Valensise, G.: Inferring the depth of
773 pre-instrumental earthquakes from macroseismic intensity data: a case-history from Northern Italy,
774 Scientific Reports, 9, 1–13, https://doi.org/10.1038/s41598-019-51966-4, 2019

https://doi.org/10.5194/egusphere-2026-2323
Preprint. Discussion started: 11 May 2026

Sbarra, P., Burrato, P., De Rubeis, V., Tosi, P., Valensise, G., Vallone, R., and Vannoli, P.: Inferring the depth and magnitude of pre-instrumental earthquakes from intensity attenuation curves, Nat. Hazards Earth Syst. Sci., 23, 1007–1028, https://doi.org/10.5194/nhess-23-1007-2023, 2023.

Scognamiglio, L., Tinti, E., and Quintiliani, M.: Time Domain Moment Tensor (TDMT) [Data set], Istituto Nazionale di Geofisica e Vulcanologia (INGV), https://doi.org/10.13127/TDMT, 2006.

Sibol, M. S., Bollinger, G. A., and Birch, J. B.: Estimation of magnitudes in central and eastern North America using intensity and felt area, B. Seismol. Soc. Am., 77(5), 1635-1654, 1987.

Sieberg, A.: Geologische, physikalische und angewandte Erdbebenkunde, G. Fischer, Jena, 1923.

Sørensen, M. B., Stromeyer, D., and Grunthal, G.: Attenuation of Macroseismic Intensity: A New Relation for the Marmara Sea Region, Northwest Turkey, B. Seismol. Soc. Am., 99, 538–553, https://doi.org/10.1785/0120080299, 2009.

Tang, Y., Lam, N., Tsang, H.-H., and Lumantarna, E.: Use of Macroseismic Intensity Data to Validate a Regionally Adjustable Ground Motion Prediction Model, Geosciences, 9, 422, https://doi.org/10.3390/geosciences9100422, 2019.

Vannoli, P., Burrato, P., and Valensise, G.: The seismotectonics of the Po Pain (Northern Italy): tectonic diversity in a blind faulting domain, Pure Appl. Geophys., 172, 1105–1142, https://doi.org/10.1007/s00024-014-0873-0, 2015.

Viganò, A., Bressan, G., Ranalli, G., and Martin, S.: Focal mechanism inversion in the Giudicarie-Lessini seismotectonic region (Southern Alps, Italy): Insights on tectonic stress and strain, Tectonophysics, 460, 106–115, https://doi.org/10.1016/j.tecto.2008.07.008, 2008.

Volatili, T., Gironelli, V., Luzi, L., Galli, P., Carafa, M. M. C., and Tondi, E.: Elusive seismogenic sources of historical earthquakes: insights from the Mw 6.8, 1706 Maiella earthquake (central Italy), Bull. Earthq. Eng., 23(4), 1279-1296, https://doi.org/10.1007/s10518-025-02110-3, 2025.

Zampieri, D., Vannoli, P., and Burrato, P.: Geodynamic and seismotectonic model of a long-lived transverse structure: The Schio-Vicenza Fault System (NE Italy), Solid Earth, 12, 1967–1986, https://doi.org/10.5194/se-12-1967-2021, 2021.

Wells, D. L. and Coppersmith, K. J.: New empirical relationships among magnitude, rupture length, rupture width, rupture area, and surface displacement, B. Seismol. Soc. Am., 84, 974–1002, 1994.